

# A Square-Wave Current Inverter for Aircraft-Mounted Electromagnetic Surveying Systems

J. A. Ferreira, Ian J. Kane, Philip Klinkert, and Teo B. Hage

**Abstract**—An inverter topology that has been developed for geophysical surveying applications makes it possible to achieve very fast current reversal in magnetic field coils. The inverter also makes it possible to generate waveforms that contain a variable high-frequency spectrum superimposed on a high-amplitude low-frequency fundamental. A feature, which is attractive from an implementation point of view, is that a low-voltage source such as a battery can be combined with high-voltage transistors to meet high dynamic requirements. Two variations of the topology are discussed, namely, a clamped and unclamped version. The proposed inverter was successfully implemented in two aircraft-mounted geophysical surveying systems achieving substantial performance improvement over the older systems. A 40-kW system was constructed for a fixed-wing aircraft and a smaller, battery-operated system was implemented on a helicopter.

**Index Terms**—Airborne geophysical surveying, magnetic field amplifier, resonant inverter, square current wave.

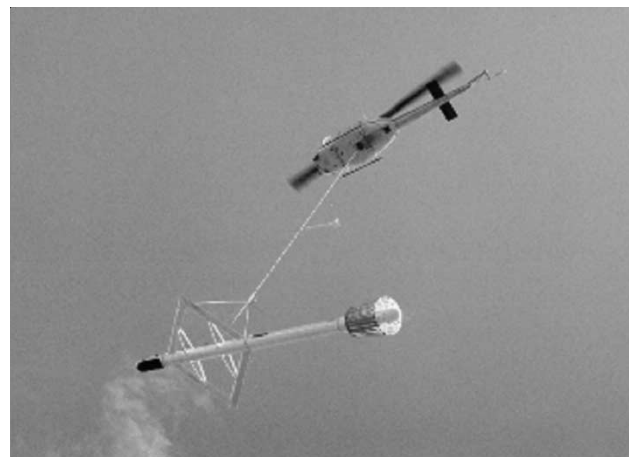
## I. INTRODUCTION

A NUMBER of applications exist where alternating magnetic fields are used to measure properties of objects. Applications range from simple metal detectors to sensing systems, such as nondestructive testing of metal surfaces [1] and flow measurements [2], magnetic resonance imaging (MRI) and geophysical surveying. In its simplest form a high- $Q$  coil is connected in series or parallel to a capacitor and is excited at the resonant frequency using an oscillator and an amplifier. In this way the coil reactance can be overcome, making it possible to generate a relatively large magnetic field for a given power source.

One of the more sophisticated systems that use electromagnetic field sensing is the aircraft-mounted electromagnetic geophysical surveying system. It comprises a current carrying coil that is wound around the perimeter of the aircraft and is attached to the nose, wing tips and the tail. An alternating current interacts with conductive or magnetic properties of rock formations



(a)



(b)

Fig. 1. Electromagnetic surveying system on a fixed-wing aircraft and a helicopter.

in the earth. The magnetic fields, emitted by the earth formation, induce a voltage in a coil that forms part of a receiver which is dragged behind the aircraft.

A new inverter topology that was developed for electromagnetic surveying is discussed in this contribution. It was implemented on the two aircraft shown in Fig. 1. The coil is the faint black lines between the nose and tail cones and the wing tips in Fig. 1(a). A helicopter drags the system shown in Fig. 1(b). The diamond shaped part at the bottom of the figure is the coil and the inverter is built into the black section on the nose.

The fixed-wing system is designed for regional ultradeep penetration geophysical surveys in relatively gentle terrain using frequencies lower than 100 Hz. Fixed-wing systems are considerably more powerful than their helicopter counterparts, and due their increased flying height and speed, a larger volume of

Paper IPCSD 03–102, presented at the 2002 Industry Applications Society Annual Meeting, Pittsburgh, PA, October 13–18, and approved for publication in the IEEE TRANSACTIONS ON INDUSTRY APPLICATIONS by the Industrial Power Converter Committee of the IEEE Industry Applications Society. Manuscript submitted for review October 15, 2002 and released for publication October 17, 2003.

J. A. Ferreira is with Electrical Power Processing, Electrical Engineering Group, Mathematics and Computer Science, Delft University of Technology, 2628 CD Delft, The Netherlands (e-mail: J.A.Ferreira@ITS.TUdelft.NL).

I. J. Kane is with Celerant Consulting, Richmond TW9 2JX, U.K.

P. S. Klinkert is with Spectrem Air Ltd., 1748 Lanseria, South Africa, and also with the Geoscience Research Group, Anglo Operations Limited, Parktown 2193, Johannesburg, South Africa (e-mail: phil@spectrem.co.za).

T. B. Hage is with Fugro Airborne Surveys, Lanseria 1748, Johannesburg, South Africa (e-mail: thage@fugroairborne.co.za).

Digital Object Identifier 10.1109/TIA.2003.821808

earth is energized and therefore they do not have the spatial resolution of helicopter-borne systems. The helicopter system can be used in severe terrain and in areas where fixed-wing systems cannot operate as a result of insufficient infrastructure. When more spatial resolution is needed a helicopter system is used as a follow-up tool for the fixed-wing system.

## II. INVERTERS USED IN OLDER SYSTEMS

In the earliest versions a resonant circuit, comprising the magnetic field coil and series connected capacitor, was excited with a thyristor bridge resulting in sinusoidal pulses with a controllable dead time. The history of the “fixed-wing towing bird” surveying system goes back to 1958 when Barringer introduced the so-called “INDuced PULse Transient” waveform and description of earlier circuits can be found in patents (for example, [3]) and is described by the acronym INPUT. It was succeeded by the so-called COTRAN arrangement where the resonant capacitor was placed in parallel instead of in series with the magnetic field coil [4]. The current waveforms have a square-wave shape with resonant transitions. The acronym COTRAN comes from COsine TRANsient. The basic working principles of the current-source inverter using forced commutation can be found in a number earlier of publications, such as [5]. Aircraft-mounted electromagnetic surveying systems have become more sophisticated during the years and a large amount of signal processing is done in real-time when flying. Square-wave currents are preferred over sinusoidal waveforms because they contain harmonics and the additional frequencies provide more information for geophysical surveying. Fast transients are desirable on the COTRAN inverters because it enhances the harmonic content of the magnetic field.

In recent years we have witnessed a dramatic improvement in fully controllable switches and the tendency has been to replace current source inverters with voltage source inverters over the broad range of power electronic converters. In line with this development a new voltage fed inverter topology for energizing magnetic field coils has been developed and is reported in this contribution.

## III. RESONANT INVERTER CIRCUIT

In most applications of inverters the load current or the load voltage stays essentially constant during a switching cycle of a power electronics converter. For example, a dc power supply delivers a direct voltage and the inverter of an electrical drive supplies a current that has a relatively small ripple superimposed on a dc current component. In this application, though, the load current is entirely ac within a cycle and the desire is to have more complicated waveforms than purely sinusoidal.

The closest topological relative of the proposed circuit is the resonant link converter [6]. What this topology has in common with our proposed topology is that both have a resonant capacitor on the dc bus that is connected to the transistor poles. One difference is that the resonant inductor has been replaced by a diode. The resonant inductor has been moved to the load in the new inverter.

Two versions of the circuit are proposed, namely, a clamped and an unclamped version and are shown in Fig. 2. A special

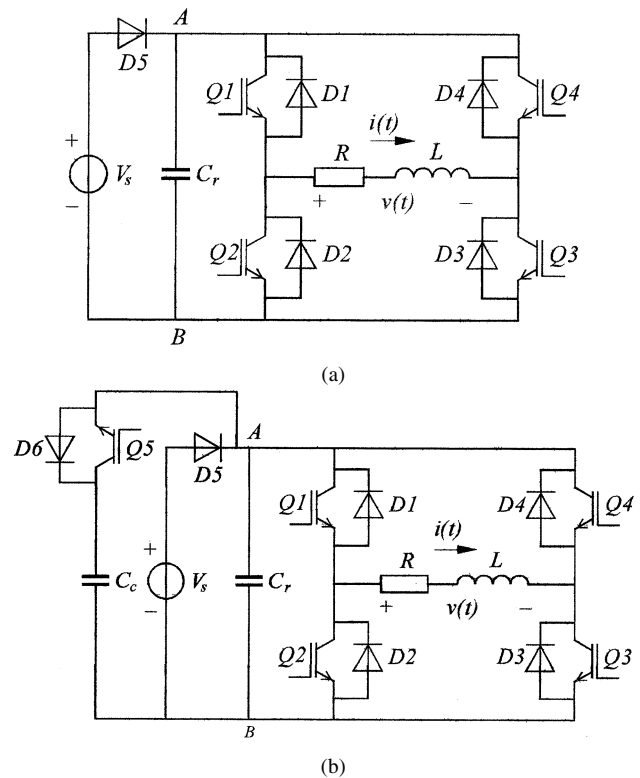


Fig. 2. Inverter for fast current reversal. (a) Unclamped topology. (b) Clamped topology.

feature of these topologies is that a transistor H-bridge is positioned between the resonant inductor and resonant capacitor. This rather unique feature gives it special control possibilities.

The proposed circuits feature two main advantages.

- The voltage used for current reversal can be made much larger than the value of the source. This implies that the current reversal can be driven by a voltage that is only limited by the breakdown voltage characteristics of the transistors and it not limited by the voltage value of the source.
- Pulsewidth modulation at high switching frequencies provides more flexibility to control the wave shape than is possible with sinus-wave resonant converters or thyristor-based inverters.

### A. Conduction Modes

Turning the inverter circuits, shown in Fig. 2, inside out one notices that the semiconductor switches and the diodes serve to connect either the voltage source  $V_s$ , the resonant capacitor  $C_r$ , or the clamping capacitor  $C_c$  to the coil, that is represented as an equivalent series circuit comprising  $R$  and  $L$ . Optionally, it is also possible to apply a short circuit across the coil, by turning on both the top switches or the bottom switches of the two phase arms.

Two types of conduction modes are possible. In the first type the current shows a first-order, or exponential, waveform behavior. This happens when the voltage source  $V_s$  or short circuit is applied across the coil. Since the clamping capacitor  $C_c$  is

very large, the voltage changes little during the conduction interval and the clamping voltage can be assumed to be a constant voltage source  $V_c$ .

The waveforms of the exponential interval are given by the following equations:

$$v(V_o, t) = V_o \quad (1)$$

$$i(V_o, I, t) = \frac{V_o}{R} + \left[ I - \frac{V_o}{R} \right] e^{-\sigma t} \quad (2)$$

where

$$\sigma = \frac{R}{L} \quad (3)$$

$V_o$  is a constant voltage 0,  $V_s$ , or  $V_c$  V, and  $I$  is the initial current in  $L$ .

Second-order behavior occurs when the coil is connected to the resonant capacitor  $C_r$ . The interval length of the conduction mode is comparable to the repetition period of the resonance between the coil inductance  $L$  and the capacitor  $C_r$ . The minimum absolute value of the voltage applied to the coil in this mode is  $V_s$ , and if a clamp is present the voltage is  $V_c$ . The current and voltage waveforms for the resonant discharge (RD) and resonant charging (RC) intervals are given by the following second-order equations:

$$v(V, I, t) = V_s + \frac{V - V_s}{\sin \phi(V, I)} e^{-\frac{\sigma t}{2}} \sin(\omega t + \phi(V, I)) \quad (4)$$

$$i(V, I, t) = \frac{C_r \omega (V - V_s)}{\sin \phi(V, I)} e^{-\frac{\sigma t}{2}} \times \left[ \cos(\omega t + \phi(V, I)) - \frac{\sigma}{2\omega} \sin(\omega t + \phi(V, I)) \right] \quad (5)$$

where

$$\phi(V, I) = \tan^{-1} \left[ \frac{-I}{C_r \omega (V - V_s)} + \frac{\sigma}{2\omega} \right]^{-1} \quad (6)$$

$$\omega = \sqrt{\frac{1}{LC_r} - \left( \frac{R}{2L} \right)^2} \quad (7)$$

and  $V$  is the initial voltage on  $C_r$ .

By using the above two basic conduction modes one can derive six different general conduction modes that can be used to compose various waveforms. They are as follows:

- a *resonant charging interval* when resonance occurs between the coil inductance and the resonant capacitor and during which the coil current is increased.;
- a *resonant discharging interval* during which the amplitude of the current is decreased;
- a *slow exponential discharging interval* when a short circuit is applied to the coil, and during which the current decays according to the  $RL$  time constant of the coil;
- a *slow exponential charging interval* during which the supply voltage,  $V_s$ , is applied to the coil, resulting in a slow exponential rise of the current;
- a *fast exponential discharging interval* during which the clamp voltage,  $V_c$ , is applied to the coil, and D6 conducts resulting in a fast exponential decay of the current;
- a *fast exponential charging interval* during which the clamp voltage,  $V_c$ , is applied to the coil and Q5 conducts, resulting in a fast exponential rise of the current.

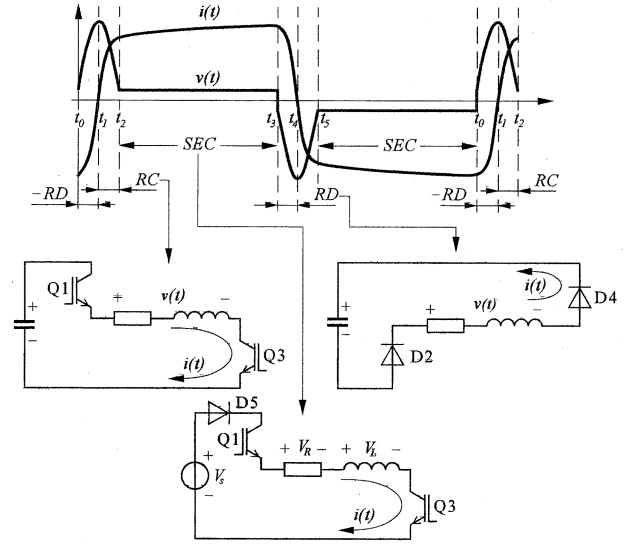


Fig. 3. Voltage and current waveforms on coil for an unclamped inverter.

### B. Unclamped Version

The circuit operation of the unclamped version is illustrated in Fig. 3, showing the coil current and the voltage appearing across it. The current waveform in this case is a square wave. During polarity reversal of current resonance occurs, the voltage  $|v(t)|$  becomes larger than  $V_s$  and the diode  $D_5$  is reversed biased, effectively decoupling the voltage source.

This interval of operation starts as soon as the pair of conducting switches (Q1 and Q3 during the positive part of the cycle and Q2 and Q4 during the negative part of the cycle) are switched off at time  $t_0$  and the diodes of the opposite pair of diagonal switches start conducting (D1 & D3). This interval is called the resonant discharge (RD) interval and ends at  $t_1$  when the energy in the coil has been discharged. At this point ( $t_2$ ) the voltage across the capacitor ( $C_r$ ) reaches a maximum and the transistors Q1 and Q3, connected in antiparallel to the diodes take over the current and energy flows from the capacitor to the inductor restoring the current, albeit in an opposite direction. This interval is called the RC interval in Fig. 3.

This resonant transition is followed by an interval during which D5 conducts and the current in the coil rises slowly. This slow exponential charging (SEC) interval follows directly after the resonant charging (RC) when the voltage across capacitor  $C_r$  reaches the voltage level of  $V_s$  and the diode D5 starts to conduct at time instant  $t_2$ . The capacitor ( $C_r$ ) now only acts as a smoothing capacitor for the voltage source and, therefore, this interval of operation shows a first-order behavior and the current wave shape is exponential depending on the  $RL$  time constant of the coil. Note that the peak voltage during the resonance interval is about an order of magnitude larger than the voltage of the source. The voltage driving the transition is not determined by the available supply voltage, but is limited by the breakdown voltage of the semiconductors.

### C. Clamped Version

The clamping conduction mode normally occurs when during when the current polarity is reversed. The operation of the clamped inverter, shown in Fig. 2(b), is similar to the

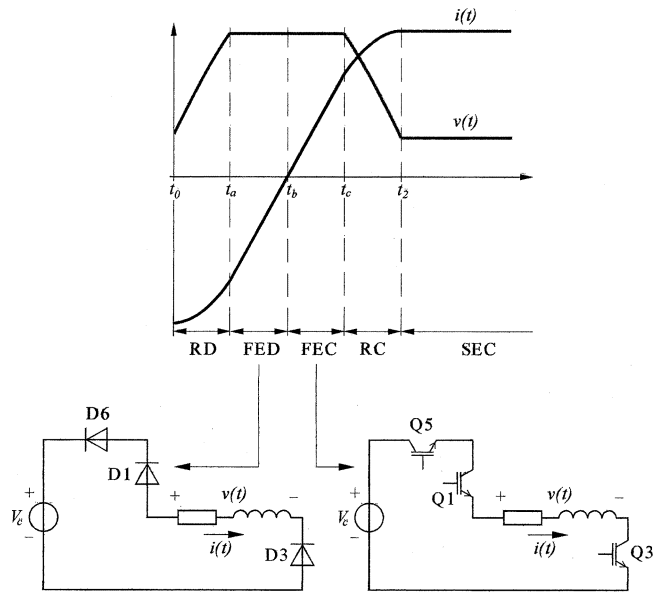


Fig. 4. Current polarity reversal of the clamped inverter.

unclamped version with the exception of the extra clamping conduction mode which occurs when Q5 or D6 conducts.

The current polarity changeover is shown in Fig. 4 and the initial conditions at  $t_0$  and subsequent resonant discharge interval corresponds with the unclamped version. However at time instant  $t_a$  the voltage across  $C_r$  reaches the value of the  $V_c$  the clamping voltage. At this point the diode D6 starts to conduct and since the capacitor  $C_c$  is very large it can be replaced by a voltage in the analysis, as can be seen in the active subcircuits indicated in Fig. 4. The clamping conduction mode is called the fast exponential discharging (FED) interval due to the fast current decay caused by the large voltage. The current changes polarity at instant  $t_b$  and the transistors Q1, Q3, and Q5 starts conducting, initiating the fast exponential charging (FEC) interval. The FEC and FED intervals can be analyzed with (1)–(3) using the clamped voltage  $V_c$ .

Q5 is turned off at  $t_c$ . This time instant is determined by a control loop that regulates the clamping voltage value. Under steady state the diode conduction interval ( $t_b - t_a$ ) and the transistor conduction intervals ( $t_c - t_b$ ) will be equal in order to achieve charge balance and stabilize the voltage on  $C_c$ .

#### IV. ELECTRONIC CONTROL OF HARMONIC CONTENT

The “COTRAN” description of the older thyristor inverter was appropriate because the waveform was fixed and the high-frequency harmonic content of the current waveform was a characteristic and controlled by this COSine TRANsient. In the proposed topology the slope of the current transient stays constant when the clamp is active resulting in a faster current reversal for a given maximum voltage rating. As a result the high-frequency content of the spectrum is enhanced. Even when the inverter is operated under unclamped conditions the extra control that the insulated gate bipolar transistors (IGBTs) give makes it possible to control the shape of the waveform and the harmonic content in a very flexible way giving more possibilities to adjust the frequency content, compared to the COTRAN thyristor inverter.

The six different conduction modes can be applied in a large number of combinations, using a microprocessor-based state

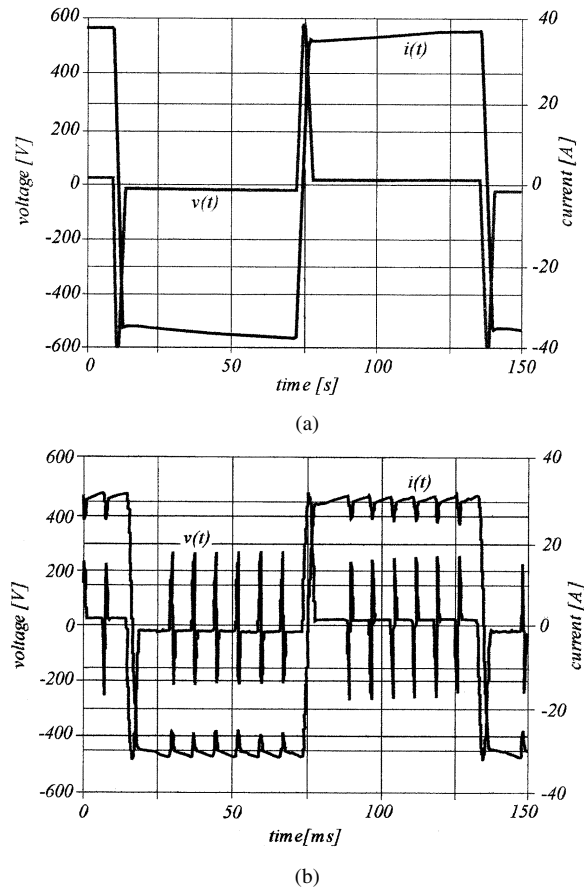


Fig. 5. Two sets of experimental coil voltage and current waveforms. (a) Flat square wave. (b) Harmonic rich square wave.

machine controller. The combination of better hardware and software makes it possible to process the reaction of the earth when subjected to more complicated waveforms, applying an increased number of frequencies at the same time. This topology, therefore, lends itself to generate harmonic rich waveforms that can be tuned to meet the specific requirements of a geophysical surveying application.

#### V. LABORATORY EXPERIMENTS

A small experimental setup was first constructed to verify the theoretical models and to test controllers. A diamond-shaped coil with a length of 4 m was suspended from the laboratory ceiling. The dimensions of the coil were scaled according to the dimensions of the fixed-wing aircraft. The coil comprised four parallel windings, each consisting of 11 series turns of copper wire with a diameter of 0.85 mm resulting in an equivalent series resistance,  $R = 0.54 \Omega$ , and inductance,  $L = 1.9 \text{ mH}$ . The inductance was experimentally measured and used to verify the equation used to design the coils of the real systems.

The inverter was constructed with IGBTs and was also a scaled-down version, operating at a lower power than the real systems. The dc source was buffered with batteries resulting in a 13-V supply voltage. The value of the resonant capacitor is  $5 \mu\text{F}$ .

In Fig. 5, experimentally measured waveforms are shown. The first waveform corresponds to the switching operation that is graphically described in Fig. 3 where only fast current re-

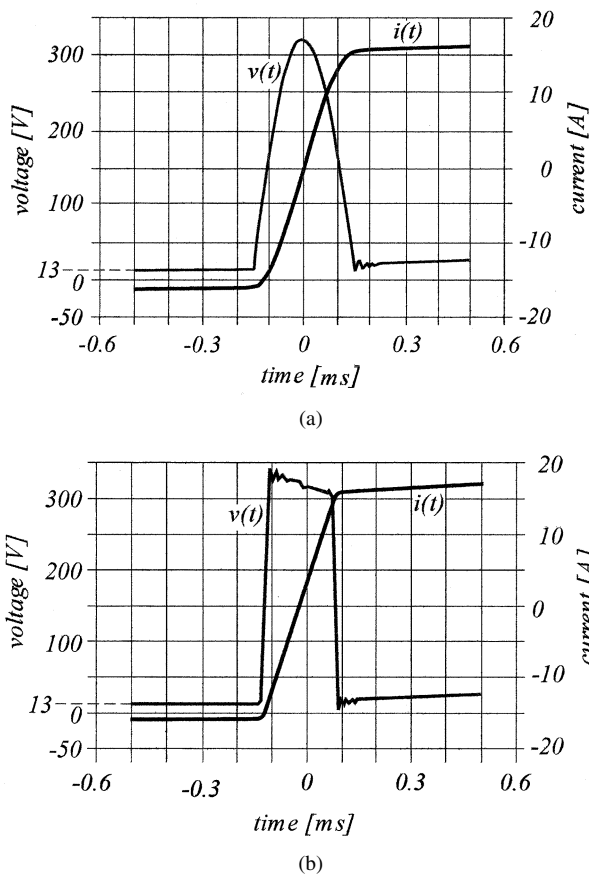


Fig. 6. Experimental waveforms of transient. (a) Unclamped topology. (b) Clamped topology.

versal is achieved and no modulation takes place at the crest of the square wave. The current has a pure square-wave form. The second waveform was generated by applying pulsewidth modulation during the positive and negative half cycles of the square wave resulting in a higher harmonic content of the waveform.

The duration of the current reversal interval determines the higher harmonic content of the waveform in the first instance. The shape of the current transient also plays a role in the higher harmonic content. The in the case of the unclamped version the transient has a smooth, cosine shape while the clamped version displays an almost constant slope during current reversal. The experimentally measured current reversal transients are shown in Fig. 6 for the unclamped and clamped versions of the circuit. For a given blocking voltage rating of the switches faster current reversal is possible with the clamped version.

The switches were operated under hard switching condition. The presence of the resonant capacitor  $C_r$  in parallel with the H-bridge takes care of possible voltage overshoots during switching transients. The average switching frequency of the inverter is lower than the inverters that are used in drives. Since we use the same semiconductor devices and modules, the switching losses will therefore be less making the inclusion of snubbers unnecessary.

## VI. IMPLEMENTATION ON THE FIXED-WING AIRCRAFT

The transmitter unit is mounted on the right-hand side of the aircraft as shown in Fig. 7. Five inverters are behind the cockpit



Fig. 7. Magnetic field transmitter unit in the fixed-wing aircraft.



Fig. 8. Five inverters in parallel.

and the rectifier and filters are in the grey box in the front and are shown in the Fig. 8.

The magnetic coil on the fixed-wing aircraft has a single turn and is wound between a special nose cone to the wing tips to a cone at the tail section. It comprises five separate conductors each having a resistance value of  $0.213 \Omega$ . The inductance of the coils has a value of  $150 \mu\text{H}$ . Each coil has its own IGBT inverter that can power square current waves up to 200 A each. It is then possible to have a maximum total current of 960 A resulting in a total rms dipole moment of  $420\,000 \text{ A}\cdot\text{m}^2$ .

The power source is a three-phase generator rated at 50 kVA. The output current is adjusted by controlling the field current to the alternator. The current as a function of the dc supply voltage is indicated in Fig. 9. A measurement of the combined current at about 80% power is shown in Fig. 10. A resonance capacitance of  $20 \mu\text{F}$  per inverter unit is dimensioned to give in a resonant voltage peak of 20 times the supply voltage and this results in a current reversal time smaller than  $200 \mu\text{s}$ .

Fig. 11 shows the spectrum of a transmitted current waveform. The base frequency in this case is 75 Hz and the spectrum is normalized with respect to this fundamental frequency resulting in 0 dB at 75 Hz. The spectrum falls off as roughly  $1/\omega$  up to 2 kHz since it is approximately a square wave. At higher harmonics the falloff is faster because the current cannot be switches as a true square wave and the current takes a finite time to reverse its polarity. The cutoff point of the  $1/\omega$  falloff rate de-

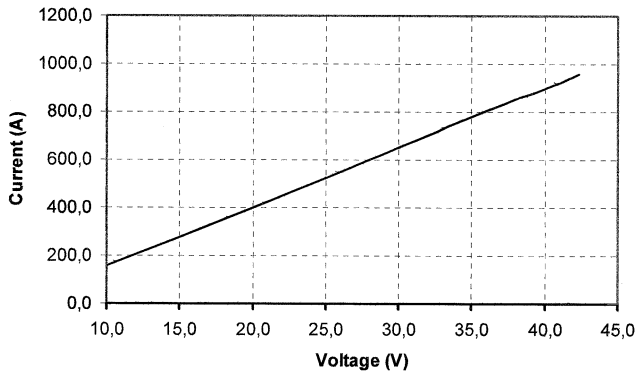


Fig. 9. Supply voltage versus loop rms current.

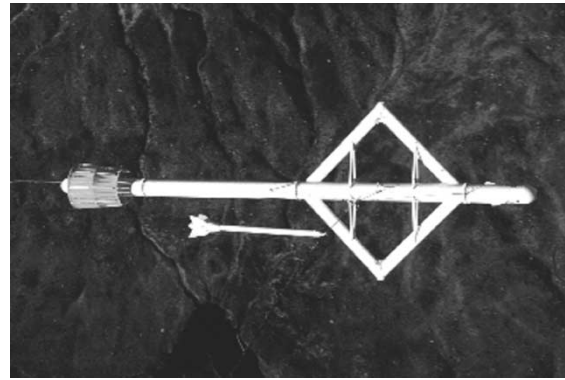


Fig. 12. Helicopter airborne electromagnetic surveying system.

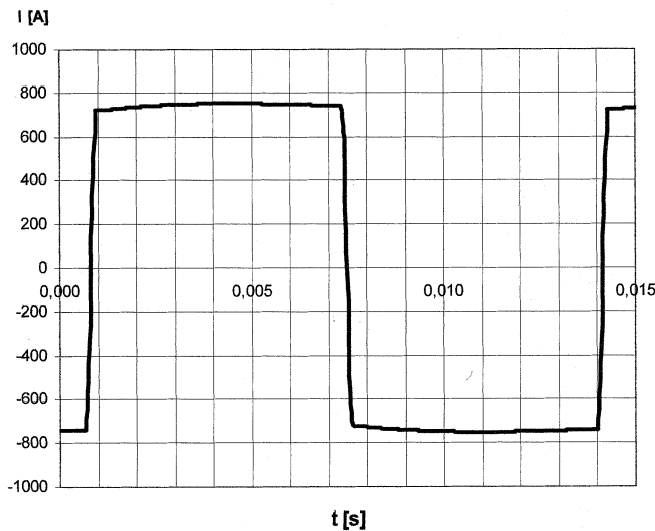


Fig. 10. Measured combined coil current waveform.

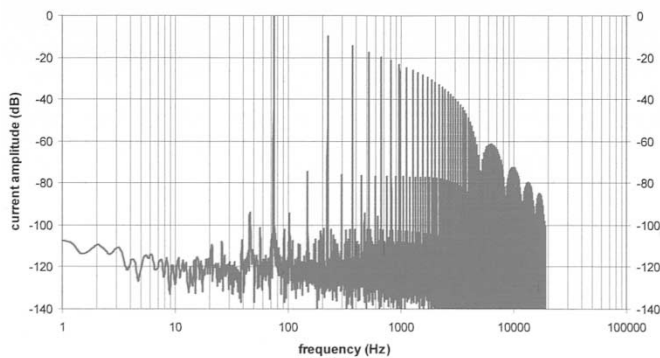


Fig. 11. Spectrum of coil current.

finer the bandwidth of the large amplitude harmonics and this has been improved substantially with the proposed topology.

The plotted spectrum is 0 beyond 20 kHz because the aliasing frequency of the A/D converter is at 19.2 kHz. While the cutoff point of the  $1/\omega$  falloff rate is determined by the available voltage that drives the current reversal, the part of the spectrum between this point and aliasing frequency is determined by the shape of the transient. In this example various lobes occur between 2 kHz–20 Hz because we have a cosine transient due to the unclamped operation in this case. When the clamped

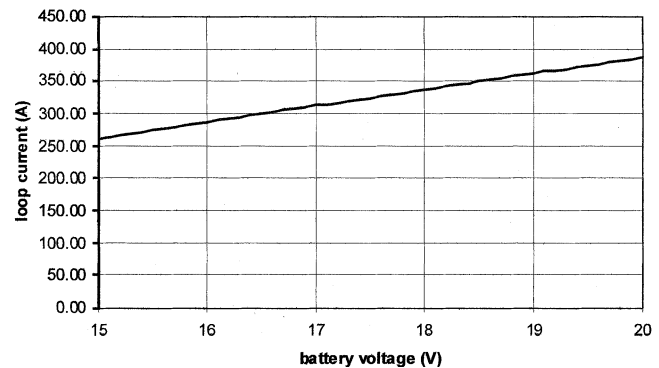


Fig. 13. Coil current as a function of battery voltage.

mode of operation is employed, the resulting current will be trapezium shaped and the spectrum will be different.

If the spectrum is perfectly symmetrical about the zero line energy will only be transmitted in the odd harmonics. However, by examining the spectrum one notices that a tiny amount of energy, about  $-80$  dB or 1 part in 10 000, is present at the even harmonics of 150 Hz, 300 Hz, and higher. This can be attributed either to an unsymmetrical layout of the bus bars used to connect the two halves of the H-bridge of the inverters, or some offset in the current sensing system.

## VII. IMPLEMENTATION ON THE HELICOPTER

In Fig. 12, a closer view of the helicopter system is shown. The diamond-shaped part forms the coil and the transmitter that includes the inverter is mounted in the nose section. The voltage is supplied from a battery and the dipole moment of up to  $20\,000\text{ A} \cdot \text{m}^2$  rms is possible.

The inverter circuit is essentially the same as the one used on the fixed-wing aircraft. The value of the loop resistance is  $40\text{ m}\Omega$ , the loop inductance is  $790\text{ }\mu\text{H}$ , and the resonant capacitor has a value of  $88\text{ }\mu\text{F}$ . The design loop current and voltage are indicated in the graph shown in Fig. 13.

## VIII. CONCLUSION

An aircraft-mounted surveying system is a specialized and unique application for a power electronics inverter. It calls for a very sharply defined square-wave current and, in this particular application, the possibility to add extra harmonic content to

the waveform was also desired. To meet these objectives a new converter topology was proposed and implemented on two aircraft. The key feature of the topology that it makes it possible have a voltage on the dc link to the inverter that can be many times higher than the dc supply voltage, which was smaller than 50 V in this application. The voltage on the dc link can be increased to match the voltage rating of modern fully controllable switches and, therefore, substantially high voltages are available to change the current of the magnetic field coil in very short times. In the airborne electromagnetic surveying systems this solution proved to be very successful and it still offers more possibilities for enriching and actively controlling the harmonic content of the magnetic field that still need to be investigated in the future.

#### REFERENCES

- [1] R. F. Mostavi and D. Mirshekar-Syahkal, "Simple electromagnetic detection of variations in properties of metal surfaces," *IEEE Trans. Magn.*, vol. 33, pp. 2492–2494, July 1997.
- [2] P. Hafner and F. Flecken, "Arrangement for generating DC magnetic field of alternating polarity for the magnetic-inductive flow measurement," U.S. Patent 4 410 926, Oct. 18, 1983.
- [3] M. Geleynse, "Pulse generator," Canadian Patent 781 000, 1966.
- [4] M. W. Paul, "Pulse generator using LC circuit to energize a coil," Canadian Patent 1 064 584, Jan. 1979.
- [5] E. E. Ward, "Inverter suitable for operation over a range of frequency," *Proc. IEEE*, vol. 111, pp. 1423–1434, Aug. 1964.
- [6] D. M. Divan, "The resonant link converter—a new concept in static power conversion," in *Conf. Rec. IEEE-IAS Annu. Meeting*, 1986, pp. 648–656.



**J. A. (Braham) Ferreira** (M'88–SM'01) was born in Pretoria, South Africa. He received the B.Sc.Eng., M.Sc.Eng., and Ph.D. degrees in electrical engineering from Rand Afrikaans University, Johannesburg, South Africa.

In 1981, he was with the Institute of Power Electronics and Electric Drives, Technical University of Aachen, and worked in industry at ESD (Pty) Ltd from 1982 to 1985. From 1986 to 1997, he was with the Faculty of Engineering, Rand Afrikaans University, where he held the Carl and Emily Fuchs Chair

of Power Electronics. Since 1998, he has been a Professor with the ITS Faculty of Delft University of Technology, Delft, The Netherlands.

Prof. Ferreira is the TRANSACTIONS Review Chairman of the Power Electronics Devices and Components Committee of the IEEE Industry Applications Society (IAS), and served as Chairman of the IEEE Joint IAS/PELS Benelux chapter and the CIGRE SC14 national committee of The Netherlands. He is also a Member of the IEEE PES AdCom, and a Member of the Executive Committee of the EPE Society.



**Ian J. Kane** received the M.B.A. degree from the University of Stellenbosch, Stellenbosch, South Africa, and the M.Eng. degree in electrical and electronics from Rand Afrikaans University, Johannesburg, South Africa.

He is a Business Analyst in the engineering field for Celerant Consulting, Richmond, U.K. He was previously a Senior Electronics Engineer with Anglo American Plc, where he was responsible for research and development of geophysical electromagnetic systems.



**Philip Klinkert** received the M.Sc. degree in geophysics from Imperial College, London, U.K., in 1972.

Since 1972, he has been with Anglo American Corporation specializing in design and development of airborne electromagnetic (AEM) systems and interpretation of data from them. He was the company project manager for the initial development of the SPECTREM fixed-wing AEM system and designed the towed bird and receiver coil suspension system for it. He is currently with the Geoscience Research

Group, Anglo Operations Limited, Johannesburg, South Africa, and mainly works as an interpreter of data collected with the SPECTREM system for base metal, gold, and diamond exploration. He is also involved in all aspects of improving the SPECTREM technology including the design of a new bird for a helicopter time-domain electromagnetic system.



**Teo B. Hage** received honors degrees in geology and geophysics and the Masters degree in applied mathematics from the University of Natal, Durban, South Africa.

He joined the Geophysical Services and Research Department of Anglo American Corporation in December 1983 as a Geophysicist. He later joined the Airborne Geophysics section. A new Airborne Electromagnetic project was initiated in 1990 and he became the General Manager of the company, Spectrem Air Ltd., Lanseria, South Africa. Since 2001, he has

also been the R&D Manager of Fugro Airborne Surveys, Lanseria, South Africa.